Acta Polytechnica CTU Proceedings **56**:23–28, 2026
https://doi.org/10.14311/APP.2026.56.0023

Published by the Czech Technical University in Prague

CALIBRATION OF THE HARDENING SOIL MODEL IN EXCALIBRE

Do Chinh Phuong*, Tomáš Kadlíček, David Mašín, Jan Najser

Charles University, Faculty of Science, Institute of Hydrogeology, Engineering Geology and Applied Geophysics, Albertov 6, 128 00 Prague 2, Czech Republic

* corresponding author: dophu@natur.cuni.cz

Abstract. The hardening soil model is one of the most commonly used constitutive models in engineering practice. This model is based on multi-surface plasticity and combines the well-known Mohr-Coulomb failure criterion, a hardening shear surface and a cap yield surface into a single model. The stress-strain behaviour is improved by including nonlinear elasticity. In this paper a calibration tool for a modified version of the hardening soil model is presented which is currently implemented in the online calibration application called *ExCalibre*.

Keywords: Hardening soil model, calibration, ExCalibre.

1. Introduction

The most commonly recognized constitutive model in engineering practice is named Mohr-Coulomb (MC) which combines Coulomb's failure criterion with Mohr's circle and thus provides a simple tool to analyse failure states of frictional materials. The basic version of this model is linked with *perfectly elastic – perfectly plastic* behaviour. Although this MC model works well in evaluating the strength of frictional materials, its deformation behaviour lacks accuracy and can be hardly relied on when the deformation response of a structure is at the centre of the analysis. This fact prompted development of new constitutive models and theories which would reliably capture this strength as well as the highly nonlinear behaviour of soils.

Aside from distinct constitutive theories such as hypoplasticity [1] and barodesy [2], the multi-surface elastoplasticity still represents a sought after group of constitutive models. A significant representative of these models is the Hardening Soil Model (HSM) [3] which, along with the MC yield surface, adopts the hardening yield surface for shearing, and then adds the additional cap yield surface which enables hardening along the hydrostatic axis. The nonlinear behaviour is defined in the terms of exponential relationships involving Young's modulus at the reference state σ^{ref}. All things considered, the HSM model gained traction among engineers and scientists for its simple definition and adequate precision in monotonic loading. However, HSM requires 10 parameters to determine its behaviour and although some of these parameters can be successfully approximated, an accurate calibration is not a simple task and requires a continuous back analysis of the parameters obtained. This task gets increasingly complicated when multiple experiments are to be calibrated simultaneously.

Therefore, a calibration application called ExCalibre [4] was developed to provides engineers and scientists alike with a convenient calibration tool which should decrease time and efforts linked with calibration work. Currently, the application allows for the calibration of the following models: hypoplastic clay [1], hypoplastic sand [5], Modified Cam Clay [6], and the Mohr-Coulomb model. Currently, ExCalibre will enable calibration of two versions of HSM models. The first version is the original version proposed by Shanz [3] whose yield surface is defined as a hexagonal pyramid and the nonlinear elasticity based on the minor stress component σ_3. The second version is implemented in the GEO5 software [7] which differs from the original version by its smooth yield surface in the deviatoric plane (Matsuoka-Nakai), and nonlinear elasticity dependent on the mean stress p. In this paper, a short comparison of these models in their essential definition, behaviour and parameters is provided and the calibration results with the modified version of the HSM [7] is shown for the sand and clay soil specimens.

2. Hardening soil models

In a sense, the HSM represents a transition between state independent constitutive models such as Mohr-Coulomb or Drucker-Prager and the models developed based on critical state soil mechanics, originally represented by the elastoplastic Cam-Clay [6] model which was later expanded upon in other theories, i.e., bounding surface plasticity [8], hypoplasticity [1] or barodesy [2].

2.1. Yield surface

The original HSM model adopts the yield surface of the MC model which is visualised by the hexagonal pyramid f_{MC} in the principal stress space, see Figure 1a. This yield surface represents the limiting envelope of all states, and one plane of the pyramid

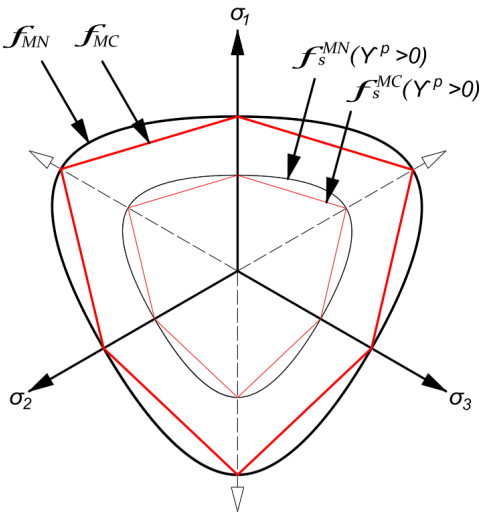

(A). Deviatoric plane.

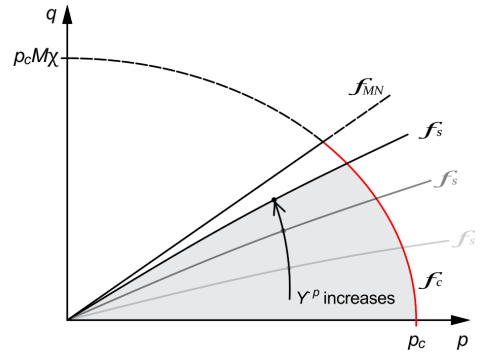

(B). Meridian plane.

Figure 1. Illustrations of the referenced yield surfaces. f_{MC} – MC yield surface, f_{MN} – Matsuoka-Nakai yield surface, f_s – shear yield surface, f_c – cap yield surface.

in the stress plane $\sigma_1 \times \sigma_3$ is defined as

$$f_{MC}(\sigma_1, \sigma_3) = \frac{1}{2}(\sigma_1 - \sigma_3) + \frac{1}{2}(\sigma_1 + \sigma_3)\sin\varphi - c\cos\varphi = 0 \quad (1)$$

with the friction angle φ and cohesion c. For other planes, the indexes are permutated from 1 to 3. However, the GEO5 version [7], implements the Matsuoka-Nakai (MN) limiting yield surface instead which is defined as

$$f_{MN} = \sin^2\varphi_m - \sin^2\varphi, \quad (2)$$

where φ_m represents a mobilized friction angle. Note that the MN surface is aligned with the MC surface at the triaxial extension and compression (corners of the pyramid) and defines increased strength at the intermediate states.

In addition to the limiting yield surface, the hardening yield surface, referred to here as the shear surface f_s, is implemented. Its definition stems from the hyperbolic law of drained triaxial tests in $q \times \varepsilon_1$ plane and its implementation thus enables an accumulation of a plastic deformation during shearing. This is a striking contrast to the MC model, which produces elastic deformations only until the yield surface f_{MC} is reached. Expansion of the shear surface f_s is controlled by the accumulated plastic shear strains γ^p which thus represents a memory variable of f_s as it can only expand, see Figure 1b. In the original model [3], the shear surface is defined in the stress plane $\sigma_1 \times \sigma_3$ as

$$f_s^{MC} = \frac{2}{E_i}\frac{(\sigma_1 - \sigma_3)}{1 - (\sigma_1 - \sigma_3)/q_a} - \frac{2(\sigma_1 - \sigma_3)}{E_{ur}} - \gamma^p, \quad (3)$$

whereas GEO5 employs the relation

$$f_s^{MN} = q - \left(1 - \frac{b}{a}\right)\left(\frac{E_i}{E_{ur}}q + \frac{2}{3\sqrt{3}}E_i\gamma^p\right). \quad (4)$$

where q is a deviatoric stress, q_a is the asymptotic deviatoric stress, E_{ur} is the unloading elastic stiffness and

$$E_i = \frac{2E_{50}}{2 - R_f}, \quad a = \frac{1 - \sin\varphi_m}{\varphi_m}, \wedge \quad b = \frac{R_f(1 - \sin\varphi)}{\sin\varphi} \quad (5)$$

being the initial elastic stiffness and shear surface coefficients, respectively. Note that E_{50} is used as a parameter of the shear surface f_s and thus does not represent an elastic property. The initial stiffness E_i assures that E_50 is reached during a shearing at 50 % of maximum deviatoric stress for the given failure ratio

$$R_f = \frac{q_a}{q_f}. \quad (6)$$

In the contrast to other common elastoplastic models, the HSM employs the unloading stiffness E_{ur} and the unloading Poisson's ratio ν_{ur} due to the fact that both the shear f_s and the cap f_c yield surfaces are active during the primary loading. The elastic parameters E_{ur} and ν_{ur} thus control the elastic unloading and reloading to the yield surfaces. The HSM thus does not enable any cyclic accumulation.

The shape of the cap yield surface f_c is inspired by the yield surface of the Modified Cam-Clay model (MCC), but however, its centre is located in the origin of the plane $p \times q$ as Figure 1b indicates. In the original version, f_c is defined as

$$f_c^{MC} = \frac{\tilde{q}^2}{M^2} + p^2 - p_c^2 \quad (7)$$

while GEO5 uses a slightly modified relation

$$f_c^{MN} = \frac{q^2}{\chi^2 M^2} + p^2 - p_c^2. \quad (8)$$

Both $\tilde{q}$ and χ assure that the values of the limiting states are reached correctly at the triaxial compression and triaxial extension and interpolates the intermediate values. The parameter M defines the height of the cap yield surface. Similarly with γ^p, the overconsolidation stress p_c serves as a memory variable of the cap yield surface f_c and marks its scale. The HSM model thus incorporates 3 yield surfaces in total as Figure 1 illustrates.

2.2. Deformation characteristics

The nonlinear elastic behaviour occurs during the unloading and reloading to the shear f_s and cap f_c yield surfaces. The unloading elastic stiffness E_{ur} of the original model [3] is defined as

$$E_{ur} = E_{ur}^{ref} \left(\frac{\sigma_3 + c\cot\varphi}{\sigma_3^{ref} + c\cot\varphi} \right)^m, \tag{9}$$

where E_{ur}^{ref} represents the unloading elastic stiffness at the reference minor stress σ_3^{ref},

$$E_{ur} = E_{ur}^{ref} \left(\frac{p + c\cot\varphi}{p^{ref} + c\cot\varphi} \right)^m, \tag{10}$$

usually $\sigma_3^{ref} = 100\,\text{kPa}$. The parameter m imposes an exponential relation on E_{ur}. During simulations of various engineering problems, such as excavations, σ_3 can suddenly change direction and cause an abrupt change in stiffness resulting in convergence issues. To remedy this problem, some versions of HSM such as GEO5 FEM replaced σ_3 dependency by the mean stress p dependency as similarly to E_{ur}, the exponential relationship for the secant stiffness modulus is defined as

$$E_{50} = E_{50}^{ref} \left(\frac{\sigma_3 + c\cot\varphi}{\sigma_3^{ref} + c\cot\varphi} \right)^m \tag{11}$$

Note that in GEO5 version, σ_3 is replaced with the mean stress p as reported in Equation (9) and Equation (10). See Figure 2 for the illustrations of these stiffnesses.

HSM models employ the non-associated flow rule of the shear surface f_s, where the mobilized dilatancy ψ_m is linked with the critical state friction angle φ_c and mobilized friction angle φ_m through Rowe's [9] dilatancy relation

$$\sin\psi_m = \frac{\sin\varphi_m - \sin\varphi_c}{1 - \sin\varphi_m \sin\varphi_c}. \tag{12}$$

The original HSM model employs MC plastic potential

$$g_{MC}(\sigma_1, \sigma_3) = \tfrac{1}{2}(\sigma_1 - \sigma_3) + \tfrac{1}{2}(\sigma_1 + \sigma_3)\sin\psi_m = 0, \tag{13}$$

whereas GEO5 employs the MN shape of the plastic potential defined as

$$g_{MN} = q + (\sigma_m - ccot\varphi)M_\psi, \text{where } M_\psi = \tfrac{6\sin\psi_m}{3-\sin\psi_m}. \tag{14}$$

In order to restrict the infinite accumulation of volumetric strains during a drained test or unrestricted increase of deviatoric stress during an undrained test, the mobilized dilatancy ψ_m is limited by the void ratio e_{max} and the critical state friction angle φ_c as

$$\sin\psi_m = 0 \quad \text{for} \quad \varphi_m < \varphi_c \wedge e < e_{max}. \tag{15}$$

The cap yield surface adopts the MCC associated flow rule, however, HSM does not implicitly define

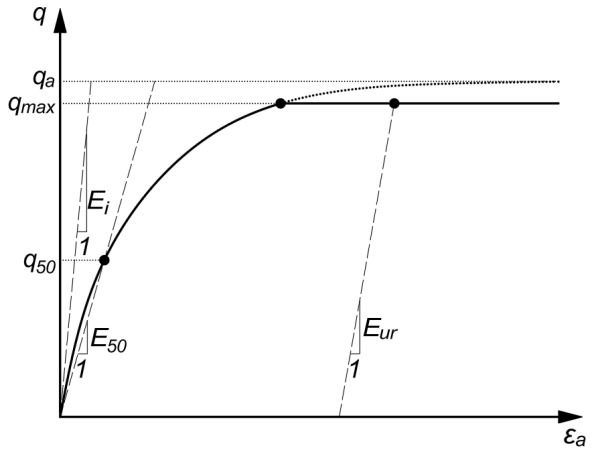

Figure 2. Stiffness representation in $q \times \varepsilon_a$. E_{50} – stiffness at q_{50}, E_i – initial stiffness, E_{ur} – unloading/reloading stiffness.

MCC's hardening rule due to the lack of the related parameters λ and κ. Expansion of f_c is thus linked with the volumetric plastic strains ε_v^p via hardening modulus H as in

$$\dot{\varepsilon}_v^p = \frac{1}{H}\dot{p}_c. \tag{16}$$

It is often mentioned that the parameters M and H should not be used as the input parameters and their values should be linked with the oedometric modulus E_{oed}^{ref} and K_0 at the reference state, meaning that the yielding of the cap must occur at the reference state. If, however, the soil is overconsolidated and p_c significantly differs from the reference stress p_{ref}, the simulated compression curve with the M and H estimates will considerably diverge from the reality.

Besides the mentioned parameters, HSM maintains these state variables:

- γ^p – accumulated plastic shear strains defined the magnitude of the shear surface f_s,
- e – void ratio is maintained to check for the dilatancy cut at e_{max},
- p_c – overconsolidation stress defines the magnitude of the cap yield surface f_c,
- φ_m – mobilised friction angle controls evolution of the mobilised dilatancy angle ψ_m,
- ψ_m – mobilised dilatancy angle.

3. Calibration

ExCalibre [4] is developed based on analytical estimations and deterministic optimization processes which follow established theories of engineering geology and critical state soil mechanics. The calibration enables simultaneous optimization of multiple laboratory experiments while maintaining fast optimization speed and provides a convenient user interface with displayed results and an option of manual recalibration according to the user's needs.

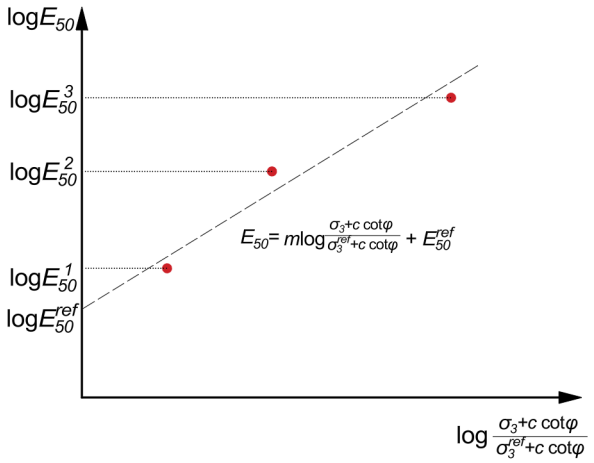

Figure 3. Evaluation of E_{50}^{ref} and m from the set of 3 drained triaxial tests.

The HSM model is defined by 10 parameters in total. Although all these parameters can be, in theory, set independently, some of these parameters are related. First, the focus is aimed at the stiffness driving parameters E_{50}^{ref}, E_{ur}^{ref}, E_{oed}^{ref}, E_i, m, ν_{ur}, and σ_{ref} (or p_{ref}). Determination of the reference secant modulus E_{50}^{ref} is straightforward once individual E_{50} from a set of drained triaxial tests are evaluated as displayed in Figure 3. E_{50}^{ref} is in this case the intersection of the regression line with the vertical axis and m is its slope. Although it is postulated that stiffnesses E_{50}, E_{ur}, and E_{oed} are evolving identically by the parameter m, it is not in general the case and a preference must be applied to either of these stiffness measures to reliably calibrate m. Recall that E_{50}^{ref} corresponds to E_{50} at the reference state, which is most often set as $\sigma_{ref} = 100\,\text{kPa}$. Importantly, the regression analysis is valid only in the case of overconsolidated soils, meaning the cap surface f_c does not interfere with the shearing, otherwise the simulated E_{50} will not correspond to the input value E_{50} and the response is softer than expected. In such a case, the optimization of E_{50} must take place to enforce the required secant stiffness E_{50}. In addition, in the previous section, it was mentioned that the hyperbolic stiffness law stems from the drained triaxial tests and thus in the case of undrained tests, the optimization also must take place to fit the laboratory data with the simulation.

The parameters E_{ur}^{ref} and ν_{ur} are purely elastic properties and although they can be calculated from the unloading path of a drained triaxial test, this section of the test is usually not available. Therefore, E_{ur}^{ref} is evaluated from the unloading path of an oedometric test at the reference stress σ_{ref} provided that ν_{ur} is known. In examined publications on HSM $\nu_{ur} = 0.2$ and therefore this value is used by default in ExCalibre. The oedometric modulus E_{oed}^{ref} is recommended to be evaluated at the reference stress and together with K_0^{NC} serve for the optimization of the parameters M and H, which are sometimes referred to as the *internal parameters*. For instance, in Plaxis, the parameters M and H (in Plaxis replaced by K_s/K_c ratio) cannot be set independently by a user and they are internally optimized so that E_{oed}^{ref} and K_0^{NC} are maintained at the reference stress σ^{ref}. To match the Plaxis internal parameters calibration, ExCalibre enables the same optimization to calibrate M and H parameters. However, M and H can be optimized not only to comply with a single value at σ_{ref} but also to better fit a whole span of compression testing. This option is also available in ExCalibre.

The strength parameters φ and c are calibrated as a regression of peak states in triaxial tests. Unlike in the MC model, HSM enables a progressive evolution of dilatancy ψ as Equation (15) suggests. In this case, the critical state friction angle φ_c is a conditional parameter which switches on the dilatancy, and it is obtained from the maximum dilatancy ψ and the peak friction angle φ as

$$\sin\varphi_c = \frac{\sin\varphi - \sin\psi}{1 - \sin\varphi\sin\psi}. \tag{17}$$

The dilatancy cut-off parameter e_{max} is calculated as the average of maximum void ratios triaxial tests. In the case of undrained tests, $e_{max} = 0$ since its averaging would cancel dilatative behaviour only at lower confining pressures.

The parameter R_f is defined as the ratio between the asymptotic deviatoric stress of hyperbolic stress-strain q_a and ultimate deviatoric stress q_f, recall Equation (6). Due to the nature of the hyperbolic relation in Equation (3), the parameter must uphold $R_f < 1$. Although in many applications it is set at default as $R_f = 0.9$, there are various approaches to its estimation [10]. Ultimately, the parameter controls the rate of stiffness degradation when approaching q_a. Similarly to E_{50} these estimates serve well when calibrating overconsolidated soils. Therefore, R_f is thus optimized in $q \times \varepsilon_1$ plane.

4. Calibration results

Two examples of calibration are presented. The first is represented by a low plasticity clay (CL), and the second is represented by well graded sand (SW). Each soil was calibrated with the GEO5 versions of HSM and, for reasons of comparison, complemented with two other constitutive models implemented in ExCalibre, namely Mohr-Coulomb (MC), hypoplastic sand (HS), and hypoplastic clay (HC). The parameters of the HSM model calibrated on the sand and clay specimens are shown in Table 1 and Table 2, respectively.

4.1. Sand

The oedometric test presented in Figure 4, with oedometer sample is of a loose initial state. The MC model, in this case, does not follow the experiment since the elastic parameters Young's modulus E and

	E_{50}^{ref}	E_u^{ref}	φ_p	C_p	ν	R_f	m_p	ψ	M	H
GEO5	67265	128124	35	45.3	0.2	0.95	0.72	10.6	1.17	4140

TABLE 1. Calibrated parameters: Sands.

	E_{50}^{ref}	E_u^{ref}	φ_p	C_p	ν	R_f	m_p	ψ	M	H
GEO5	48338	101766	25	23.2	0.2	0.99	0.3	3.3	1.32	5419

TABLE 2. Calibrated parameters: Clay.

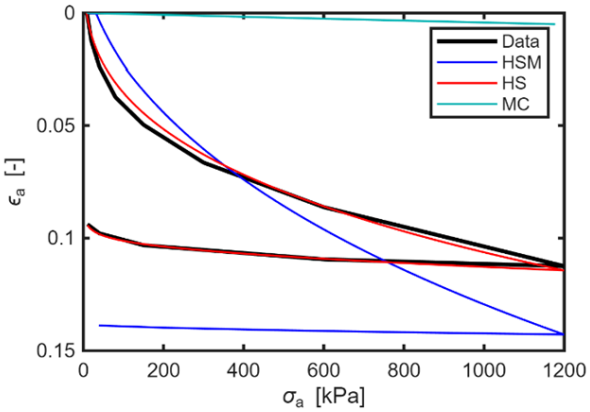

FIGURE 4. Oedometric test.

Poisson's ratio ν are calibrated on the drained triaxial test. The HSM parameters H and M of the cap yield surface f_c are calibrated to obtain the lateral coefficient at the rest K_0 and Young's modulus in oedometric conditions E_{oed} at the reference stress $p_{ref} = 100\,\text{kPa}$. The oedometric curve presented by the HSM follows the experiment much closer than the MC model. The last simulation is presented by the hypoplastic sand model, which is based on critical state soil mechanics and qualitatively follows the oedometric experiment much more closely.

Results of the drained triaxial tests are displayed in Figure 5. The shear stiffness of the MC model results from the average E_{50}. The HSM evaluates individual E_{50} based on the parameters E_{50}^{ref} and m. In this case, a relatively high R_f shows a reasonable rate of stiffness degradation when approaching the peak states. Dilatancy ψ is in both cases calculated alike as the average of dilatancies corresponding to individual drained triaxial tests. Noteworthy is the dilatancy cut-off presented by the HSM model in comparison with the MC model. The hypoplastic sand follows well the stiffness degradation when approaching the peak states and reasonably follows the subsequent softening. The dilatancy of the hypoplastic model is exaggerated, which is a commonly known drawback of this model.

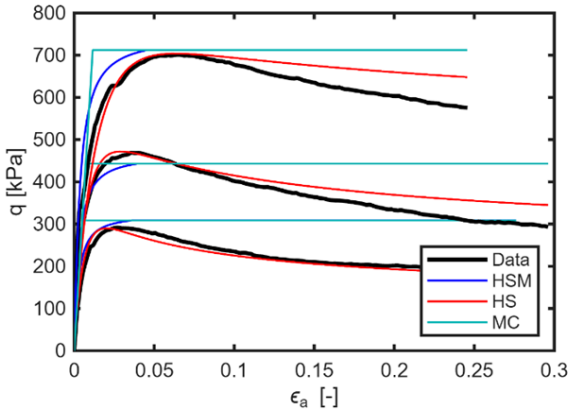

(A). $q \times \varepsilon_a$.

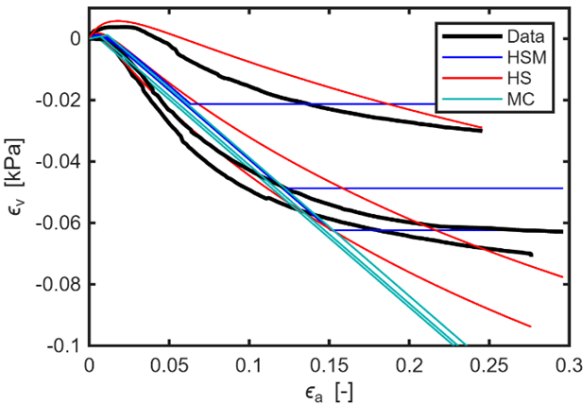

(B). $\varepsilon_v \times \varepsilon_a$.

FIGURE 5. Drained triaxial tests.

4.2. CLAY

Similarly to the previous example, the MC model does not follow the underlying oedometric experiment, see Figure 6. Although the HSM model follows the experiment more closely, the hypoplastic clay model matches the experiment very well.

The optimized shear stiffness of the MC model in undrained conditions is shown in Figure 7 with the bilinear diagram. The HSM model shows a degree of nonlinearity with the influence of the dilatancy. Notice the evolution of these two models in $p \times q$ space, where MC model undergoes an elastic behaviour until its yield surface is reached while the HSM model

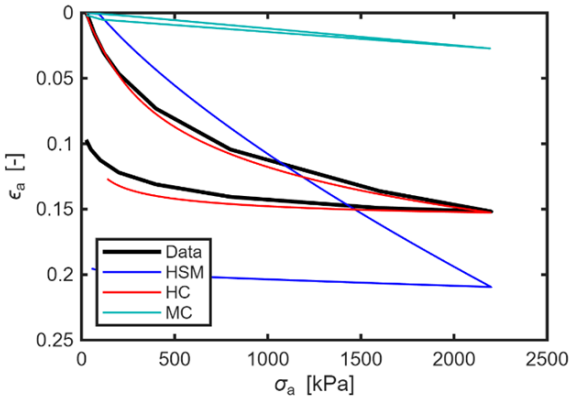

Figure 6. Oedometric test.

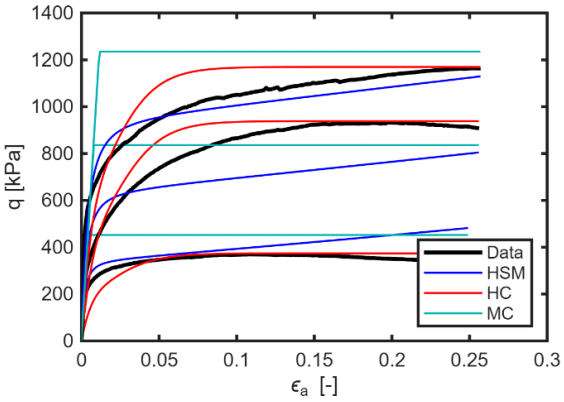

(a). $q \times \varepsilon_a$.

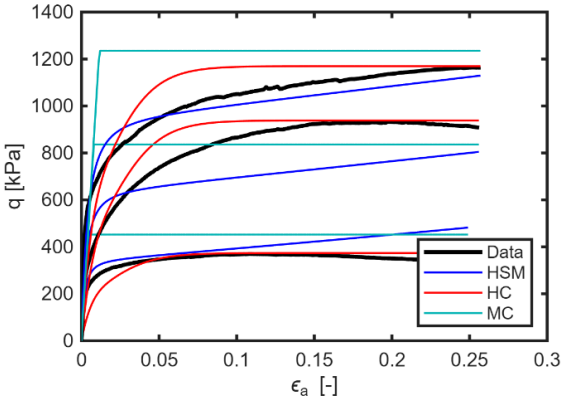

(b). $q \times p$.

Figure 7. Undrained triaxial tests.

shows a distinct contractive behaviour followed with a dilatancy at the yield surface f_{MN}. The hypoplatic clay model follows relatively well the experiments in $q \times \varepsilon_a$ plane while its performance is not that significant in the $q \times p$ due to a low initial stiffness. This is a known draw-back of hypoplastic models which is remedied with a small-stain extension.

5. Conclusion

In this contribution, preliminary calibration results of the hardening soil model were presented alongside three other already implemented constitutive models. ExCalibre provides not only automated calibration, but it also allows manual recalibration if more specific tuning of the calibration is preferred. Publishing the calibration for both the original [3] and modified versions [7] of the HSM model is planned during 2025.

Acknowledgements

The authors acknowledge financial support from the research grant GACR 22-12178S. The third author acknowledges financial support given by the Center for Geosphere Dynamics (UNCE/SCI/006).

References

[1] D. Mašín. Clay hypoplasticity with explicitly defined asymptotic states. *Acta Geotechnica* **8**:481–496, 2013. https://doi.org/10.1007/s11440-012-0199-y

[2] G. Medicus, W. Fellin, D. Kolymbas. Barodesy for clay. *Géotechnique Letters* **2**(4):173–180, 2012. https://doi.org/10.1680/geolett.12.00037

[3] T. Schanz, P. A. Vermeer, P. G. Bonnier. The hardening soil model: Formulation and verification. In *Beyond 2000 in Computational Geotechnics*, pp. 281–296. Routledge, 2019.

[4] T. Kadlíček, T. Janda, M. Šejnoha, et al. Automated calibration of advanced soil constitutive models. Part I: hypoplastic sand. *Acta Geotechnica* **17**:3421–3438, 2022. https://doi.org/10.1007/s11440-021-01441-0

[5] P. V. Wolffersdorff. A hypoplastic relation for granular materials with a predefined limit state surface. *Mechanics of Cohesive-frictional Materials: An International Journal on Experiments, Modelling and Computation of Materials and Structures* (3):251–271, 1996.

[6] K. H. Roscoe, J. B. Burland. On the generalized stress/strain behaviour of wet clay. In J. Hayman, F. A. Lockhead (eds.), *Engineering Plasticity*, pp. 535–609. Cambridge University Press, 1968.

[7] Fine spol. s r.o. GEO5 Software FEM, 2025. [2026-02-10]. https://www.finesoftware.eu/geotechnical-software/fem/

[8] A. L. Petalas, Y. F. Dafalias, A. G. Papadimitriou. SANISAND-F: Sand constitutive model with evolving fabric anisotropy. *International Journal of Solids and Structures* **188-189**:12–31, 2020. https://doi.org/10.1016/j.ijsolstr.2019.09.005

[9] P. W. Rowe. The stress-dilatancy relation for static equilibrium of an assembly of particles in contact. In *Proceedings of the Royal Society of London. Series A. Mathematical and Physical Sciences 269.1339*, pp. 500–527. 1962.

[10] Y. Fu, S. He, S. Zhang, Y. Yang. Parameter analysis on hardening soil model of soft soil for foundation pits based on shear rates in Shenzhen Bay, China. *Advances in Materials Science and Engineering* **2020**(1):7810918, 2020. https://doi.org/10.1155/2020/7810918